

1 **Particle acidity and sulfate production during severe haze events in China**  
2 **cannot be reliably inferred by assuming a mixture of inorganic salts**

3  
4 Gehui Wang<sup>1,2,3,\*</sup>, Fang Zhang<sup>4,5</sup>, Jianfei Peng<sup>5,6</sup>, Lian Duan<sup>5,7</sup>, Yuemeng Ji<sup>5,8</sup>, Wilmarie  
5 Marrero-Ortiz<sup>5</sup>, Jiayuan Wang<sup>2</sup>, Jianjun Li<sup>2</sup>, Can Wu<sup>2</sup>, Cong Cao<sup>2</sup>, Yuan Wang<sup>9</sup>, Jun Zheng<sup>10</sup>,  
6 Jeremiah Secrest<sup>5</sup>, Yixin Li<sup>5</sup>, Yuying Wang<sup>4,5</sup>, Hong Li<sup>11</sup>, Na Li<sup>5,12</sup>, and Renyi Zhang<sup>5,6\*</sup>

7  
8 <sup>1</sup>Key Laboratory of Geographic Information Science of the Ministry of Education, School of  
9 Geographic Sciences, East China Normal University, Shanghai 200241, China

10 <sup>2</sup>State Key Laboratory of Loess and Quaternary Geology, Institute of Earth Environment, China  
11 Academy of Sciences, Xi'an 710061, China

12 <sup>3</sup>Center for Excellence in Regional Atmospheric Environment, Institute of Urban Environment,  
13 Chinese Academy of Science, Xiamen, China

14 <sup>4</sup>Beijing Normal University, Beijing 100875, China

15 <sup>5</sup>Departments of Atmospheric Sciences and Chemistry, Texas A&M University, College Station,  
16 TX, 77843, USA

17 <sup>6</sup>State Key Joint Laboratory of Environmental Simulation and Pollution Control, College of  
18 Environmental Sciences and Engineering, Peking University, Beijing 100871, China

19 <sup>7</sup>East China University of Science and Technology, Shanghai, China

20 <sup>8</sup>School of Environmental Science and Engineering, Institute of Environmental Health and  
21 Pollution, Control, Guangdong University of Technology, Guangzhou 510006, China

22 <sup>9</sup>Jet Propulsion Laboratory, California Institute of Technology, Pasadena, CA 91125, USA

23 <sup>10</sup>Jiangsu Key Laboratory of Atmospheric Environment Monitoring and Pollution Control,  
24 Nanjing University of Information Science & Technology, Nanjing 210044, China

25 <sup>11</sup>State Key Laboratory of Environmental Criteria and Risk Assessment, Chinese Research  
26 Academy of Environmental Sciences, Beijing 100012, China

27 <sup>12</sup>Key Laboratory of Songliao Aquatic Environment, Jilin Jianzhu University, Changchun,  
28 130118, China

29  
30  
31  
32  
33 \*Corresponding author:

34 Prof. Gehui Wang, E-mail : [ghwang@geo.ecnu.edu.cn](mailto:ghwang@geo.ecnu.edu.cn), or [wanggh@ieecas.cn](mailto:wanggh@ieecas.cn)

35 Prof. Renyi Zhang, E-mail: [renyi-zhang@tamu.edu](mailto:renyi-zhang@tamu.edu)

37 **Abstract:** Atmospheric measurements showed rapid sulfate formation during severe haze  
38 episodes in China, with fine particulate matter (PM) consisting of a multi-component mixture  
39 that is dominated by organic species. Several recent studies using the thermodynamic model  
40 estimated the particle acidity and sulfate production rate, by treating the PM exclusively as a  
41 mixture of inorganic salts dominated by ammonium sulfate and neglecting the effects of organic  
42 compounds. Noticeably, the estimated pH and sulfate formation rate during pollution periods in  
43 China were highly conflicting among the previous studies. Here we show that a particle mixture  
44 of inorganic salts adopted by the previous studies does not represent a suitable model system and  
45 that the acidity and sulfate formation cannot be reliably inferred without accounting for the  
46 effects of multi-aerosol compositions during severe haze events in China. Our laboratory  
47 experiments show that SO<sub>2</sub> oxidation by NO<sub>2</sub> with NH<sub>3</sub> neutralization on fine aerosols is  
48 dependent on the particle hygroscopicity, phase-state, and acidity. Ammonium sulfate and oxalic  
49 acid seed particles exposed to vapors of SO<sub>2</sub>, NO<sub>2</sub>, and NH<sub>3</sub> at high relative humidity (RH)  
50 exhibit distinct size growth and sulfate formation. Aqueous ammonium sulfate particles exhibit  
51 little sulfate production, in contrast to aqueous oxalic acid particles with significant sulfate  
52 production. Our field measurements demonstrate significant contribution of water-soluble  
53 organic matter to fine PM in China and indicate that the use of oxalic acid in laboratory  
54 experiments is representative of ambient organic dominant aerosols. While the particle acidity  
55 cannot be accurately determined from field measurements or calculated using the  
56 thermodynamic model, our results reveal that the pH value of ambient organics-dominated  
57 aerosols is sufficiently high to promote efficient SO<sub>2</sub> oxidation by NO<sub>2</sub> with NH<sub>3</sub> neutralization  
58 under polluted conditions in China.

59

60

## 61 1. Introduction

62 Atmospheric measurements have demonstrated rapid sulfate production during severe haze  
63 events in China (Guo et al., 2014; Wang et al., 2014; Zhang et al., 2015; Cheng et al., 2016;  
64 Wang et al., 2016). For example, Wang et al. (2016) showed that during pollution episodes in  
65 Xi'an of China the  $\text{SO}_4^{2-}$  mass concentration increased markedly from less than 10, 10-20, to  
66 greater than  $20 \mu\text{g m}^{-3}$ , with the corresponding increases in the mean  $\text{PM}_{2.5}$  mass concentrations  
67 from 43, 139, to  $250 \mu\text{g m}^{-3}$  from clean, transition, to polluted periods, respectively. Among the  
68  $\text{PM}_{2.5}$  species in Xi'an, organic matter (OM), nitrate ( $\text{NO}_3^-$ ), and  $\text{SO}_4^{2-}$  were most abundant, with  
69 the mass fractions of 55%, 14%, and 14%, respectively, during the polluted period. In addition,  
70 the work by Wang et al. (2016) demonstrated that the molar ratio of  $\text{SO}_4^{2-}$  to  $\text{SO}_2$ , which reflects  
71 sulfur partitioning between the particle and gas phases, exhibited an exponential increase with  
72 relative humidity (RH), with the values of less than 0.1 at  $\text{RH} < 20\%$  to 1.1 at  $\text{RH} > 90\%$  in  
73 Xi'an. Similar evolutions in  $\text{SO}_4^{2-}$  mass concentrations and the molar ratio of  $\text{SO}_4^{2-}$  to  $\text{SO}_2$  were  
74 shown during the pollution development in Beijing (Sun et al., 2013; Wang et al., 2014; Wang et  
75 al., 2016). The rapid sulfate formation measured in China could not be explained by current  
76 atmospheric models and suggested missing sulfur oxidation mechanisms (Wang et al., 2014).  
77 Typically, high sulfate levels during haze events in China occurred concurrently with elevated  
78 RH,  $\text{NO}_x$ , and  $\text{NH}_3$  (Wang et al., 2014; Zhang et al., 2015; Wang et al., 2016), implicating an  
79 aqueous sulfur oxidation pathway. On the basis of complementary field and experimental  
80 measurements, Wang et al. (2016) concluded that the aqueous oxidation of  $\text{SO}_2$  by  $\text{NO}_2$  is key to  
81 efficient sulfate formation, but is only feasible under two atmospheric conditions, i.e., on fine  
82 aerosols with high RH and  $\text{NH}_3$  neutralization or under cloud conditions.

83 Several recent studies estimated the particle acidity and aqueous sulfate production during

84 severe haze events in China using the thermodynamic model (Cheng et al., 2016; Guo et al.,  
85 2017; Liu et al., 2017). For example, Cheng et al. (2016) estimated a pH range of 5.4 to 6.2 using  
86 a thermodynamic model (ISORROPIA-II) in Beijing. On the basis of their estimated pH and the  
87 previous experimental rates of SO<sub>2</sub> oxidation by NO<sub>2</sub> and the Henry's Law constants for sulfur  
88 dioxide (SO<sub>2</sub>), bisulfite (HSO<sub>3</sub><sup>-</sup>), and sulfite (SO<sub>3</sub><sup>2-</sup>) from the literature (Lee and Schwartz, 1983;  
89 Clifton et al., 1988; Seinfeld and Pandis, 2006), the authors derived a sulfate production rate and  
90 concluded that reactive nitrogen chemistry in aerosol water explained the sulfate formation  
91 during polluted periods in Beijing. In contrast, other recent studies by Guo et al. (2017) and Liu  
92 et al. (2017) adopted the similar method as Cheng et al. (2016), but reported significantly  
93 different values of pH and the sulfate formation rates by the aqueous SO<sub>2</sub> oxidation by NO<sub>2</sub> in  
94 China. Those two later studies determined a pH range of 3.0-4.9 and suggested that fine particles  
95 were moderately acidic and the aqueous SO<sub>2</sub> oxidation by NO<sub>2</sub> was unimportant during severe  
96 wintertime haze periods in China.

97 In this article, we conducted laboratory measurements of the hygroscopicity for oxalic acid  
98 particles and particle growth of ammonium sulfate particles upon exposure to SO<sub>2</sub>, NO<sub>2</sub>, and  
99 NH<sub>3</sub> at high RH conditions, in order to evaluate the dominant factors regulating the aqueous  
100 oxidation of SO<sub>2</sub> by NO<sub>2</sub>. In addition, field measurements of chemical compositions of water-  
101 soluble fraction for fine PM (including oxalic acid) in Beijing, Hebei Province, and Xi'an of  
102 China were performed during the winter haze episodes, showing significantly enriched water-  
103 soluble organic matter (WSOM). The implications for the multi-aerosol chemical compositions  
104 on the pH value and sulfate production during winter pollution periods in China are discussed.

## 105 **2. Methods**

### 106 **2.1 Aqueous phase oxidation of SO<sub>2</sub> by NO<sub>2</sub> in an environmental chamber**

107 The experimental method using the environmental chamber has been discussed elsewhere  
108 (Wang et al., 2016), and here we only provide a brief description. The aqueous SO<sub>2</sub> oxidation  
109 experiments was conducted by exposing size-selected (NH<sub>4</sub>)<sub>2</sub>SO<sub>4</sub> seed particles to different  
110 levels of SO<sub>2</sub>, NO<sub>2</sub>, and NH<sub>3</sub> at variable RH conditions in a 1 m<sup>3</sup> Teflon reaction chamber  
111 covered with aluminum foil. A differential mobility analyzer (DMA) equipped with a  
112 condensation particle counter (CPC) was used to measure the particle growth in diameter, in  
113 order to determine sulfate formation on seeded particles (Wang et al., 2016).

## 114 **2.2 Measurement of hygroscopic growth factor of oxalic acid**

115 Hygroscopic growth factor (HGF) of oxalic acid was measured according to the method  
116 previously discussed (Khalizov et al., 2009; Pagels et al., 2009). Briefly, a hygroscopicity  
117 tandem differential mobility analyzer (HTDMA) coupled to a condensation particle counter  
118 (CPC, TSI 3762) was used for the HGF measurement. Size-selected oxalic acid particles with the  
119 dry diameter of 100 nm were exposed to increasing RH from 8% to 92% with a step range from  
120 1%-10%. HGF is defined as the ratio of oxalic acid particle diameter ( $D_p$ ) measured by the  
121 second DMA at an elevated RH to the initial diameter ( $D_0 = 100$  nm) of the particles selected by  
122 the first DMA at the dry conditions of RH = 8% (Peng et al., 2016).

## 123 **2.3 Chemical composition of PM<sub>2.5</sub> in Beijing, Hebei Province, and Xi'an, China**

124 PM<sub>2.5</sub> samples were collected onto pre-baked (450°C for 6 hr) quartz fiber filter by using a  
125 high-volume air sampler with an airflow rate of 1.03 m<sup>3</sup> min<sup>-1</sup>. The sample collection in Xi'an  
126 was performed on the roof of a three-story building in the urban center with a 1-hour interval for  
127 each sample during the winter of 2012 (Wang et al., 2016). The sample collection in Beijing was  
128 conducted during the winter of 2016 on the roof of a four-story building on the campus of China  
129 Research Academy of Environmental Sciences, which is located at the northern part of Beijing.

130 The PM<sub>2.5</sub> samples in Hebei Province were collected during the winter of 2016 on the roof of a  
131 three-story building on the campus of the Institute of Hydrology and Environmental Geology,  
132 which is located in Zhengding County of Hebei Province. Both sample collections in Beijing and  
133 Hebei Province were performed on a day/night basis. After collection, all samples were sealed  
134 individually in an aluminum foil bag and stored in a freezer below -18°C prior to analysis.  
135 During the sampling periods temperatures were  $-6.0 \pm 4.0$  °C (-15–1.0°C),  $-4.0 \pm 3.0$  °C (-  
136 12–2.0°C) and  $1.6 \pm 4.4$  °C (-5.4–15°C) in Beijing, Hebei Province and Xi’an, respectively, while  
137 relative humidity at the three sites (RH) were  $37 \pm 18\%$  (16–87%),  $46 \pm 21\%$  (16–87%) and  $59 \pm$   
138  $21\%$  (15–95%), respectively. Previous observations showed that coal combustion, biomass  
139 burnings and vehicle exhausts are the three major sources of PM<sub>2.5</sub> during winter in North China  
140 including Beijing, Hebei Province and Xi’an (Li et al., 2016; Zhang et al., 2015).

141 The detailed procedures for the analysis of inorganic ions and water-soluble organic matter  
142 (WSOM) in aerosols have been reported elsewhere (Wang et al., 2009; Wang et al., 2010; Wang  
143 et al., 2017). Briefly, one part of the filter sample (area about 5 cm<sup>2</sup>) was divided into several  
144 pieces, extracted with Milli-Q pure water, and determined for WSOM and inorganic ions by  
145 using Shimadzu TOC-L CPH analyzer and Dionex-600 ion chromatography, respectively.  
146 Oxalic acid in PM<sub>2.5</sub> was analyzed according to Wang et al. (2002) and Cheng et al. (2015). One  
147 part of the filter sample was extracted with Milli-Q water, concentrated to dryness, and reacted  
148 with 14% BF<sub>3</sub>/butanol at 100°C for 1 hr. After the reaction, the derivatized sample was extracted  
149 with hexane for three times and concentrated into 1 mL. Oxalic acid in the samples was  
150 identified by gas chromatography–mass spectrometry (GC–MS) and quantified by gas  
151 chromatography (Agilent GC7890A).

### 152 **3. Results**

### 153 3.1 Aqueous oxidation of SO<sub>2</sub> by NO<sub>2</sub> with NH<sub>3</sub> neutralization

154 We first evaluated the factors controlling the aqueous phase oxidation of SO<sub>2</sub> by NO<sub>2</sub> using  
155 the environmental chamber method. The evolution in the size of ammonium sulfate particles  
156 after exposure to SO<sub>2</sub>, NO<sub>2</sub>, and NH<sub>3</sub> at different RH and SO<sub>2</sub> levels is shown in Figure 1. In our  
157 experiments, monodisperse particles with the initial dry particle size ranging from 50 to 70 nm  
158 were selected for the exposure, and two different SO<sub>2</sub> concentrations (37.5 and 375 parts per  
159 billions or ppb) were used. RH was maintained at a level of 80-98%, above the deliquescence  
160 point (79%) of ammonium sulfate (Qiu and Zhang, 2013) to ensure aqueous particles. As is  
161 shown in Figure 1, the size of (NH<sub>4</sub>)<sub>2</sub>SO<sub>4</sub> particles remains nearly invariant (within the  
162 experimental uncertainty) after exposure to SO<sub>2</sub>, NO<sub>2</sub>, and NH<sub>3</sub>. A 10-fold increase in the SO<sub>2</sub>  
163 concentration has little effect on the growth of (NH<sub>4</sub>)<sub>2</sub>SO<sub>4</sub> particles. These results illustrate that  
164 sulfate production is insignificant and SO<sub>2</sub> cannot be efficiently oxidized by NO<sub>2</sub> in the presence  
165 of NH<sub>3</sub> on aqueous ammonium sulfate particles. The measurement of negligible growth for  
166 (NH<sub>4</sub>)<sub>2</sub>SO<sub>4</sub> particles exposed to SO<sub>2</sub>, NO<sub>2</sub>, and NH<sub>3</sub> at high RH is in contrast to the previous  
167 work by Wang et al. (2016), which showed large size growth and significant sulfate production  
168 for oxalic acid particles with NH<sub>3</sub> neutralization and under high RH conditions (see the black  
169 triangles in Figure 1).

170 To gain an insight into such a difference in the size growth between (NH<sub>4</sub>)<sub>2</sub>SO<sub>4</sub> and oxalic  
171 acid particles, we measured the hygroscopic growth of oxalic acid particles. Figure 2 displays the  
172 measured hygroscopic growth factor (HGF) of oxalic acid, showing an exponential increase with  
173 an increase in RH. The measured HGF value is close to unity at RH < 40% and increases from  
174 1.1 at RH = 60% to 1.5 at RH = 90%. Our measured HGF for oxalic acid is consistent with the  
175 previous studies by Prenni et al. (2001) and Mikhailov et al. (2009); all of which were measured

176 by using a hygroscopicity tandem differential mobility analyzer (HTDMA) system. On the other  
177 hand, another earlier experimental study showed little growth for oxalic acid particles under high  
178 RH conditions by using an electrodynamic balance (EDB) system (Peng et al., 2001). The  
179 different HGF measured for oxalic acid is most likely due to the different accuracies of the two  
180 types of methods for the hygroscopicity measurement. The measurements of HGF also provide  
181 information on the particle phase-state. As evident from Figure 2, oxalic acid particles mainly  
182 exist in a non-aqueous phase at  $RH < 40\%$  but in the aqueous phase at  $RH > 60\%$ .

183 Our present experiments of aqueous oxidation of  $SO_2$  by  $NO_2$  were performed at similar  
184 conditions as those by Wang et al. (2016), i.e., with comparable concentrations for  $SO_2$ ,  $NO_2$ ,  
185 and  $NH_3$  and in the same phase-state (aqueous) for the particles. On the other hand, the particle  
186 acidity is clearly distinct between the two studies. Our present experiment is characterized by a  
187 lower pH value, since ammonium sulfate is rather acidic. For example, the pH value of 0.1M  
188  $(NH_4)_2SO_4$  solution is 5.5. The overall aqueous reaction between  $SO_2$  and  $NO_2$  in the presence of  
189  $NH_3$  is suggested as the following (Wang et al., 2016),



191 Since the solubility of  $SO_2$  decreases markedly with increasing particle acidity (Seinfeld and  
192 Pandis, 2006; Zhang et al., 2015), the heterogeneous reaction between  $SO_2$  and  $NO_2$  is prohibited  
193 on acidic  $(NH_4)_2SO_4$  particles. On the other hand, under the experimental conditions by Wang et  
194 al. (2016), the heterogeneous reaction between oxalic acid and  $NH_3$  occurred on aqueous  
195 particles in the presence of  $NH_3$ , yielding ammonium oxalate. The ammonium oxalate is  
196 expected to be less acidic than ammonium sulfate, because for a bulk solution the pH value of  
197 0.1 M ammonium oxalate is 6.5 and one unit higher than that of ammonium sulfate. As a result,  
198  $SO_2$  readily dissolves into aqueous ammonium oxalate particles and is oxidized by  $NO_2$  into



199  $\text{SO}_4^{2-}$ , which is consequently neutralized by  $\text{NH}_3$  to produce  $(\text{NH}_4)_2\text{SO}_4$ . The resulting aqueous  
200 ammonium oxalate/ $(\text{NH}_4)_2\text{SO}_4$  particles, which is internally mixed, exhibit a lower acidity than  
201 that of pure  $(\text{NH}_4)_2\text{SO}_4$  particles, responsible for a significant growth in the dry particle size and  
202 sulfate formation for the previous experiments by Wang et al. (2016).

203 Hence, the experimental studies of our present work and that by Wang et al. (2016) reveal  
204 that sulfate production on fine particles is dependent on several factors, including the particle  
205 hygroscopicity, phase-state, acidity, and RH, in addition to the gaseous concentrations of  $\text{SO}_2$ ,  
206  $\text{NO}_2$ , and  $\text{NH}_3$ . These experimental results indicate that the acidity and sulfate formation are  
207 distinct for organic seed and ammonium sulfate seed particles. While oxidation of  $\text{SO}_2$  by  $\text{NO}_2$   
208 on aqueous  $(\text{NH}_4)_2\text{SO}_4$  particles does not represent a viable mechanism because of a higher  
209 acidity, significant sulfate production occurs on oxalic acid particles because of a lower acidity.

### 210 **3.2 Field measurements of WSOM in China**

211 Atmospheric measurements have shown that the occurrence of severe haze episodes in  
212 China is accompanied with high RH conditions and  $\text{PM}_{2.5}$  particles consist of large amounts of  
213 secondary organic and inorganic compounds. We present additional field measurements of the  
214 chemical composition of  $\text{PM}_{2.5}$  in Beijing, Hebei Province, and Xi'an of China. Figure 3 shows  
215 that the wintertime  $\text{PM}_{2.5}$  samples collected at the three locations. It is evident that WSOM is  
216 considerably enriched and their concentrations are comparable to those of the total inorganic ions  
217 (Figure 3a and b). For example, the mass concentration of WSOM ranges from 10 to  $60 \mu\text{g m}^{-3}$   
218 in Beijing and Hebei Province during the winter of 2016 and from 10 to  $180 \mu\text{g m}^{-3}$  in Xi'an  
219 during the winter of 2012 (Figure 3c and d, respectively). Compared to those in Beijing and  
220 Hebei Province, the more abundant WSOM in Xi'an was caused by more emissions from  
221 biomass burning for house heating (Li et al., 2016). As seen in Figure 3c–f, the variation of

222 WSOM displays a temporal pattern similar to that of oxalic acid, with a linear correlation  
223 coefficient of 0.79, 0.88 and 0.72 in Beijing, Hebei Province, and Xi'an, respectively (Figure 3e  
224 and f). The mass concentration of oxalic acid in fine PM during the haze episodes is about 500  
225  $\text{ng m}^{-3}$  in Beijing and Hebei Province (Figure 3e) and more than 2000  $\text{ng m}^{-3}$  in Xi'an (Figure 3f).  
226 Hence, our field measurements indicate that oxalic acid represents one of the most abundant  
227 WSOM in the aerosol-phase. Oxalic acid is a secondary product formed from the aqueous-phase  
228 oxidation of water-soluble organic precursors and ubiquitously exists in the troposphere. Like  
229 other pollutants, oxalic acid has been also shown to occur with large abundance in China (Wang  
230 et al., 2012; Cheng et al., 2013; Meng et al., 2014; Kawamura and Bikkina, 2016). As shown in  
231 Figure 3g and h, during the field observation periods sulfate at the three sites showed a temporal  
232 variation pattern similar to that of oxalic acid with a robust linear correlation ( $r^2=0.67, 0.84$  and  
233  $0.61$  in Xi'an, Beijing and Hebei Province, respectively). Such a correlation was also reported by  
234 other researchers (Wang et al, 2017, Yu et al, 2005), suggesting the cooccurrence and internally  
235 mixing state of both compounds in the atmosphere. In addition, the previous field measurements  
236 also revealed that WSOM in China is not only enriched in carboxylic acids (including oxalic acid)  
237 but also in other organic species, including carbonyls, amines, and water-soluble nitrogen-  
238 containing organic compounds (Wang et al., 2010, 2013; Zheng et al., 2015; Yao et al., 2016;  
239 Liu et al., 2017). The dominant organic acids and bases indicate that haze particles in China are  
240 multi-component in nature and the estimations of the particle acidity (or pH) and the sulfate  
241 production rate need to take into account of the effects of organic species, in addition to  
242 inorganic ions.

#### 243 **4. Discussions**

244 Several recent studies using the thermodynamic models (Wexler and Clegg, 2002;

245 Fountoukis and Nenes, 2007) estimated the particle acidity and sulfate production during  
246 pollution episodes in China (Cheng et al., 2016; Guo et al., 2017; Liu et al., 2017). Those  
247 previous studies treated the PM exclusively as a mixture of inorganic salts dominated by  
248 ammonium sulfate and neglected the effects due to the presence of organic compounds.  
249 Apparently, the conclusions by those modeling studies hinge on the validity of several critical  
250 assumptions in their analyses, including the application of the thermodynamic model, the  
251 accuracy in determining the aerosol water content (AWC), and the applicability of the earlier  
252 experimental measurements for the aqueous oxidation of SO<sub>2</sub> by NO<sub>2</sub> to atmospheric conditions.

253 Estimation of the pH values using the thermodynamic models is typically of considerable  
254 uncertainty, because of several intricate difficulties. For example, the ISORRPIA-II model  
255 includes two modes, i.e., metastable (aerosols are assumed to be in the liquid-phase only and  
256 may reach supersaturation) and stable (aerosols are assumed in the liquid- and solid phases that  
257 are in equilibrium) (Guo et al., 2017). Since the thermodynamic model is established on the basis  
258 of the equilibrium principles, its application to non-equilibrium conditions needs to be rigorously  
259 assessed. Also, the phase (e.g., liquid, amorphous, or crystalline) and mixing state of ambient  
260 aerosols are highly complex because of the presence of multi-component organic and inorganic  
261 species (Qiu and Zhang, 2013; Zhang et al., 2015), inevitably rendering high uncertainty in the  
262 thermodynamic calculations.

263 Guo et al. (2017) suggested that the pH predictions using the metastable mode would be  
264 more reliable than that using the stable mode, on the basis of model evaluation from measured  
265 and predicted NO<sub>3</sub><sup>-</sup> and NH<sub>4</sub><sup>+</sup> during the winter of 2012 in Xi'an. Figure 4 compares the  
266 concentrations of NH<sub>3</sub> (g) and aerosol species predicted by ISORROPIA-II with the field  
267 measurements under the metastable and stable modes in Xi'an during the winter of 2012. As

268 evident in Figure 4a and b,  $\text{NH}_3$  predicted is similar to the measured value with the metastable or  
269 stable mode. Furthermore, the predicted concentrations of  $\text{NO}_3^-$  and  $\text{NH}_4^+$  using both the  
270 metastable and stable modes are nearly identical (Fig. 4c-f). Guo et al. (2017) only compared the  
271 liquid  $\text{NH}_4^+$  and  $\text{NO}_3^-$  predicted by the model under the stable mode with the field measured  
272 aerosols composed of both liquid and solid compounds, and thus their predicted concentrations  
273 were lower than those of the measurements (see Figure S1 in Guo et al, 2017). As a result, their  
274 statement that pH prediction with the metastable mode would be more reliable than that with the  
275 stable mode was unjustified. Noticeably, the pH values estimated by the ISORROPIA-II model  
276 under the two modes are significantly different, with the values of  $4.57 \pm 0.40$  under the  
277 metastable mode and  $6.96 \pm 1.33$  under the stable mode. Most recently, it was suggested that the  
278 large discrepancy in predicting pH is attributable to the model code errors (Song et al., 2018).

279 In addition, the pH estimation by the thermodynamic model is highly dependent on the ratio  
280 of the concentration of hydrogen ions in the liquid-phase to AWC. Guo et al. (2017) and Liu et al.  
281 (2017) assumed negligible particle water associated with the organic aerosol mass. Such an  
282 assumption is clearly invalid since aerosols typically contain a large portion of WSOM in China  
283 (Fig. 3), including organic nitrogen species (Wang et al., 2010, 2013) and acids (Wang et al.,  
284 2006, 2009, 2010). Also, organic acids engage in particle-phase reactions with the basic species  
285 (i.e.,  $\text{NH}_3$  and amines), significantly enhancing the particle hygroscopicity and reducing the  
286 acidity (Gomez-Hernandez et al., 2016). In addition, because of their strong basicity and high  
287 abundance, amines likely play a key role in reducing the particle-acidity in China (Wang et al.,  
288 2010a, b; Qiu et al., 2011; Qiu and Zhang, 2012; Dong et al., 2013; Zheng et al., 2015; Yao et al.,  
289 2016; Liu et al., 2017). Consequently, the acidity for organics-dominated aerosols is  
290 considerably different from that of ammonium sulfate aerosols, as demonstrated in our

291 experimental results. While effort has been made to account for the effects of organic species on  
292 the aerosol properties (Clegg et al., 2013), the available thermodynamic models are still  
293 inadequate in representing complex multi-component aerosols. An inconsistency of the  
294 ammonium–sulfate ratios using the thermodynamic models was identified in the eastern US, also  
295 suggesting a possible role for organic species (Silvern et al., 2017).

296 Furthermore, the chemical mechanism leading to the aqueous conversion of SO<sub>2</sub> to sulfate  
297 by NO<sub>2</sub> is not well understood. The previous modeling studies adopted the aqueous reaction rate  
298 constants previously measured (Lee and Schwartz, 1983; Clifton et al., 1988), while the  
299 applicability of the earlier experimental studies to atmospheric conditions is uncertain. For  
300 example, Lee and Schwartz (1983) examined the oxidation of S(IV) by NO<sub>2</sub> in the liquid phase  
301 by flowing gaseous NO<sub>2</sub> through a NaHSO<sub>3</sub> solution at a constant pH by regulating NaOH and  
302 determined the rate constant of  $1.4 \times 10^5 \text{ M}^{-1} \text{ s}^{-1}$  at pH = 5 and with a lower limit of  $2 \times 10^6 \text{ M}^{-1} \text{ s}^{-1}$   
303 <sup>1</sup> at pH = 5.8 and 6.4 from measuring the electrical conductivity of the solution. Clifton et al.  
304 (1988) measured the rate constant for the reaction of NO<sub>2</sub> with S(IV) over the pH range of 5.3-13,  
305 by producing NO<sub>2</sub> from irradiation of NaNO<sub>2</sub> and N<sub>2</sub>O solutions and mixing with Na<sub>2</sub>SO<sub>3</sub>  
306 solutions, and obtained the second-order rate constant of  $1.24 \times 10^7$  and  $2.95 \times 10^7 \text{ M}^{-1} \text{ s}^{-1}$  from  
307 the decay of NO<sub>2</sub> monitored by absorption spectroscopy. The results of the measured rate  
308 constants between the two earlier experimental measurements differed by 1-2 orders of  
309 magnitude (Lee and Schwartz, 1983; Clifton et al., 1988). Also, both kinetic experiments  
310 employed bulk solutions and did not account for the gaseous uptake process (Lee and Schwartz,  
311 1983; Clifton et al., 1988).

312 Wang et al. (2016) obtained the SO<sub>2</sub> uptake coefficient for sulfate production from  
313 combined field measurements and laboratory experiments, and their laboratory experiments

314 using aqueous oxalic acid particles reproduced the rapid sulfate production measured under  
315 polluted ambient conditions in China. The SO<sub>2</sub> uptake coefficient on oxalic acid particles in the  
316 laboratory reaction chamber is  $8.3 \pm 5.7 \times 10^{-5}$  (Wang et al., 2016) under the humid conditions and  
317 similar to that ( $4.5 \pm 1.1 \times 10^{-5}$ ) (Wang et al., 2016) observed in Beijing during the haze period of  
318 2015. The results of the SO<sub>2</sub> uptake coefficients determined by Wang et al. (2016) are also  
319 consistent with the modeling studies in quantification of the sulfate formation using atmospheric  
320 models in the country (e.g., Wang et al., 2014), indicating the applicability of their proposed  
321 mechanism to haze conditions in China. On the other hand, Liu et al. (2017) invoked the  
322 experimental work by Hung et al. (2015) as a plausible cause for rapid SO<sub>2</sub> oxidation by O<sub>2</sub> in  
323 the absence of photochemistry, but without noting the high acidity as a necessary condition in  
324 that experimental work (i.e., pH  $\leq$  3). Most recently, Li et al. (2018) suggested an indirect  
325 mechanism of SO<sub>2</sub> oxidation by NO<sub>2</sub> via HONO/NO<sub>2</sub><sup>-</sup> produced in fast-hydrolytic  
326 disproportionation of NO<sub>2</sub> on the surface of NaHSO<sub>3</sub> aqueous microjets. In addition, another  
327 recent theoretical work by Zhang et al. (2018) indicated that under weakly acidic and neutral  
328 conditions (pH  $\leq$  7) the oxidation of HOSO<sub>2</sub><sup>-</sup> by dissolved NO<sub>2</sub> is a self-sustaining process,  
329 where the produced *cis*-HONO, HSO<sub>4</sub><sup>-</sup> and H<sub>2</sub>SO<sub>4</sub> promote the tautomerization from HSO<sub>3</sub><sup>-</sup> to  
330 HOSO<sub>2</sub><sup>-</sup> as the catalysts.

## 331 **5. Conclusions**

332 In this paper we have presented experimental measurements of the growth of ammonium  
333 sulfate seed particles exposed to vapors of SO<sub>2</sub>, NO<sub>2</sub>, and NH<sub>3</sub> at variable RH, the HGF of oxalic  
334 acid particles, and field measurements of WSOM for PM<sub>2.5</sub> during the severe haze events in  
335 Beijing, Hebei Province, and Xi'an of China. Our experimental results reveal that sulfate  
336 production on fine particles is dependent on the particle hygroscopicity, phase-state, and acidity,

337 as well as RH. The acidity and sulfate formation for ammonium sulfate seed particles are distinct  
338 from those of oxalic acid seed particles. Aqueous ammonium sulfate particles show negligible  
339 growth because of low pH, in contrast to aqueous oxalic acid particles with significant dry-size  
340 increase and sulfate formation because of high pH. In addition, our atmospheric measurements  
341 show significant concentrations of WSOM (including oxalic acid) in fine PM, indicating multi-  
342 component haze particles in China. Our results reveal that a particle mixture of inorganic salts  
343 adopted by the previous studies using the thermodynamic model does not represent a suitable  
344 model system and that the particle acidity and aqueous sulfate formation rate cannot be reliably  
345 inferred without accounting for the effects of multi-chemical compositions during severe haze  
346 events in China. Our combined experimental and field measurements corroborate the earlier  
347 finding that sulfate production via the particle-phase reaction involving SO<sub>2</sub> and NO<sub>2</sub> with NH<sub>3</sub>  
348 neutralization occurs efficiently on organics-dominated aerosols (Wang et al., 2016) but are in  
349 contradiction to the most recent studies using the thermodynamic model (Guo et al., 2017; Liu et  
350 al., 2017).

351 In conclusion, while the particle acidity or pH cannot be accurately determined from  
352 atmospheric field measurements or calculated using the thermodynamic models, our combined  
353 experimental and field results provide the compelling evidence that the pH value of ambient  
354 organics-dominated particles is sufficiently high to promote SO<sub>2</sub> oxidation by NO<sub>2</sub> with NH<sub>3</sub>  
355 neutralization under polluted conditions in China.

### 356 **Acknowledgements**

357 Financial support for this work was provided by National Key R&D Plan (Quantitative  
358 Relationship and Regulation Principle between Regional Oxidation Capacity of Atmospheric and  
359 Air Quality (No. 2017YFC0210000), the China National Natural Science Funds for

360 Distinguished Young Scholars (No.41325014), the program from National Nature Science  
361 Foundation of China (No. 41773117). This work was also supported by the Robert A. Welch  
362 Foundation (Grant A-1417) W.M.-O. was supported by the National Science Foundation  
363 Graduate Research Fellowship Program.

364



365 **References**

- 366 Cheng, C., Wang, G., Zhou, B., Meng, J., Li, J., Cao, J., and Xiao, S.: Comparison of  
367 dicarboxylic acids and related compounds in aerosol samples collected in Xi'an, China  
368 during haze and clean periods, *Atmospheric Environment*, 81(0), 443-449, 2013.
- 369 Cheng, C., Wang, G., Meng, J., Wang, Q., Cao, J., Li, J., and Wang, J.: Size-resolved airborne  
370 particulate oxalic and related secondary organic aerosol species in the urban atmosphere of  
371 Chengdu, China, *Atmospheric Research*, 161–162, 134-142, 2015.
- 372 Cheng, Y., Zheng, G., Wei, C., Mu, Q., Bo Zheng, Wang, Z., Gao, M., Zhang, Q., He, K.,  
373 Carmichael, G., Pöschl, U., and Su, H.: Reactive nitrogen chemistry in aerosol water as a  
374 source of sulfate during haze events in China, *Science Advances*, 2, e1601530, 2016.
- 375 Clegg, S.L., Qiu, C., Zhang, R.: The deliquescence behaviour, solubilities, and densities of  
376 aqueous solutions of five methyl- and ethyl-aminium sulphate salts, *Atmospheric  
377 Environment*, 73, 1-14, 2013.
- 378 Clifton, C. L., Altstein, N., and Huie, R. E.: Rate constant for the reaction of nitrogen dioxide  
379 with sulfur(IV) over the pH range 5.3-13, *Environmental Science & Technology*, 22, 586-  
380 589, 1988.
- 381 Dong, X. L., Liu, D. M., and Gao, S. P.: Seasonal variations of atmospheric heterocyclic  
382 aromatic amines in Beijing, China, *Atmospheric Research*, 120, 287-297, 2013.
- 383 Fountoukis, C., and Nenes, A.: ISORROPIA II: A computationally efficient thermodynamic  
384 equilibrium model for  $K^+$ - $Ca^{2+}$ - $Mg^{2+}$ - $NH_4^+$ - $Na^+$ - $SO_4^{2-}$ - $NO_3^-$ - $Cl^-$ - $H_2O$  aerosols, *Atmospheric  
385 Chemistry and Physics*, 7, 4639-4659, 2007.
- 386 Gomez-Hernandez, M., McKeown, M., Secret, J., Marrero-Ortiz, W., Lavi, A., Rudich, Y.,  
387 Collins, D. R., and Zhang, R.: Hygroscopic characteristics of alkylammonium carboxylate  
388 Aerosols, *Environmental Science & Technology*, 50, 2292-2300, 2016.
- 389 Guo, H., Weber, R. J., and Nenes, A.: High levels of ammonia do not raise fine particle pH  
390 sufficiently to yield nitrogen oxide-dominated sulfate production, *Scientific Reports*, 7,  
391 12109, doi:12110.11038/s41598-12017-11704-12100, 2017.
- 392 Guo, H., Liu, J., Froyd, K. D., Roberts, J. M., Veres, P. R., Hayes, P. L., Jimenez, J. L., Nenes,  
393 A., and Weber, R. J.: Fine particle pH and gas–particle phase partitioning of inorganic  
394 species in Pasadena, California, during the 2010 CalNex campaign, *Atmospheric Chemistry  
395 and Physics*, 17, 5703-5719, 2017.
- 396 Guo, S., Hu, M., Zamora, M. L., Peng, J. F., Shang, D. J., Zheng, J., Du, Z. F., Wu, Z., Shao, M.,  
397 Zeng, L. M., Molina, M. J., and Zhang, R. Y.: Elucidating severe urban haze formation in  
398 China, *Proceedings of the National Academy of Sciences of the United States of America*,  
399 111, 17373-17378, 2014.
- 400 Hung, H.-M., and Hoffman, M. R.: Oxidation of gas-phase SO<sub>2</sub> on the surfaces of acidic  
401 microdroplets: Implications for sulfate and sulfate radical anion formation in the  
402 atmospheric liquid phase, *Environmental Science & Technology*, 49, 13768-13776, 2015.
- 403 Kawamura, K., and Bikina, S.: A review of dicarboxylic acids and related compounds in  
404 atmospheric aerosols: Molecular distributions, sources and transformation, *Atmospheric  
405 Research*, 170, 140-160, 2016.
- 406 Khalizov, A.F., Zhang, R., Zhang, D. Xue, H., Pagels, J., and McMurry, P.H.: Formation of  
407 highly hygroscopic aerosols upon internal mixing of airborne soot particles with sulfuric  
408 acid vapor, *Journal of Geophysical Research-Atmospheres*, 114, D05208,  
409 doi:10.1029/2008JD010595, 2009.

410 Lee, Y. N., and Schwartz, S. E.: Kinetics of oxidation of aqueous sulfur (IV) by nitrogen  
411 dioxide, in Precipitation scavenging, dry deposition, and resuspension, edited by H. R.  
412 Pruppacher, R. G. Semmon and W. G. N. Slinm, Elsevier, New York, 1983.

413 Li, J., Wang, G., Ren, Y., Wang, J., Wu, C., Han, Y., Zhang, L., Cheng, C., and Meng, J.:  
414 Identification of chemical compositions and sources of atmospheric aerosols in Xi'an, inland  
415 China during two types of haze events, *Science of the Total Environment*, 566-567, 230-237,  
416 2016..

417 Li, L., Hoffmann, M. R., and Colussi, A. J.: The role of nitrogen dioxide in the production of  
418 sulfate during Chinese haze-aerosol episodes, *Environmental Science & Technology* 52,  
419 DOI: 10.1021/acs.est.7b05222, 2018.

420 Liu, F., Bi, X., Zhang, G., Peng, L., Lian, X., Lu, H., Fu, Y., Wang, X., Peng, P. a., and Sheng,  
421 G.: Concentration, size distribution and dry deposition of amines in atmospheric particles of  
422 urban Guangzhou, China, *Atmospheric Environment*, 171, 279-288, 2017.

423 Liu, M., Song, Y., Zhou, T., Xu, Z., Yan, C., Zheng, M., Wu, Z., Hu, M., Wu, Y., and Zhu, T.:  
424 Fine particle pH during severe haze episodes in Northern China, *Geophysical Research*  
425 *Letters*, 44, 5213-5221 ,doi: 5210.1002/2017GL073210, 2017.

426 Meng, J., Wang, G., Li, J., Cheng, C., Ren, Y., Huang, Y., Cheng, Y., Cao, J., and Zhang, T.:  
427 Seasonal characteristics of oxalic acid and related SOA in the free troposphere of Mt. Hua,  
428 central China: Implications for sources and formation mechanisms, *Science of the Total*  
429 *Environment*, 493, 1088-1097, 2014.

430 Mikhailov, E., Vlasenko, S., Martin, S. T., Koop, T., and Poeschl, U.: Amorphous and crystalline  
431 aerosol particles interacting with water vapor: conceptual framework and experimental  
432 evidence for restructuring, phase transitions and kinetic limitations, *Atmospheric Chemistry*  
433 *and Physics*, 9, 9491-9522, 2009.

434 Pagels, J., McMurry, P.H., Khalizov, A.F., and Zhang, R.: Processing of soot by controlled  
435 sulphuric acid and water condensation—Mass and mobility relationship, *Aerosol Science &*  
436 *Technology*, 43, 629–640, 2009.

437 Peng, J., Hu, M., Guo, S., Du, Z., Zheng, J., Shang, D., Zamora, M.L., Zeng, L., Shao, M., Wu,  
438 Y., Zheng, J., Wang, Y., Glen, C.R., Collins, D.R., Molina, M.J., and Zhang, R.: Markedly  
439 enhanced absorption and direct radiative forcing of black carbon under polluted urban  
440 environments, *Proceedings of the National Academy of Sciences of the United States of*  
441 *America*, 113, 4266–4271, 2016.

442 Peng, C., Chan, M. N., and Chan, C. K.: The hygroscopic properties of dicarboxylic and  
443 multifunctional acids: measurements and UNIFAC predictions, *Environmental Science &*  
444 *Technology*, 35, 4495-4501, 2001.

445 Prenni, A. J., DeMott, P. J., Kreidenweis, S. M., Sherman, D. E., Russell, L. M., and Ming, Y.:  
446 The effects of low molecular weight dicarboxylic acids on cloud formation, *Journal of*  
447 *Physical Chemistry A*, 105, 11240-11248, 2001.

448 Qiu, Q., Wang, L., Lal, V., Khalizov, A.F., and Zhang, R.: Heterogeneous chemistry of  
449 Alkylamines on Ammonium Sulfate and Ammonium Bisulfate, *Environmental Science &*  
450 *Technology*, 45, 4748–4755, 2011.

451 Qiu, C., and Zhang, R.: Physiochemical Properties of Alkylaminium Sulfates: Hygroscopicity,  
452 Thermostability, and Density, *Environmental Science & Technology*, 46, 4474-4480, 2012.

453 Qiu, C., and Zhang, R. Y.: Multiphase chemistry of atmospheric amines, *Physical Chemistry*  
454 *Chemical Physics*, 15(16), 5738-5752, 2013.

455 Seinfeld, J. H., and Pandis, S. N., *Atmospheric Chemistry and Physics: From Air Pollution to*

456 *Climate Change, 2nd ed.*, John Wiley & Sons, Hoboken, NJ, 2006.

457 Silvern, R.F., Jacob, D.J., Kim, P.S., Marais, E.A., Turner, J. R., Campuzano-Jost, P., and  
458 Jimenez, J. L. Inconsistency of ammonium–sulfate aerosol ratios with thermodynamic  
459 models in the eastern US: a possible role of organic aerosol, *Atmospheric Chemistry and*  
460 *Physics*, 17, 5107–5118, 2017.

461 Song, S., Gao, M., Xu, W., Shao, J., Shi, G., Wang, S., Wang, Y., Sun, Y., and McElroy, M. B.:  
462 Fine particle pH for Beijing winter haze as inferred from different thermodynamic  
463 equilibrium models, *Atmospheric Chemistry and Physics Discussions*,  
464 <https://doi.org/10.5194/acp-2018-6>, 2018.

465 Sun, Y. L., Wang, Z. F., Fu, P. Q., Yang, T., Jiang, Q., Dong, H. B., Li, J., and Jia, J. J.: Aerosol  
466 composition, sources and processes during wintertime in Beijing, China, *Atmospheric*  
467 *Chemistry and Physics*, 13(9), 4577-4592, 2013.

468 Wang, G., Xie, M., Hu, S., Tachibana, E., and Kawamura, K.: Dicarboxylic acids, metals and  
469 isotopic compositions of C and N in atmospheric aerosols from inland China: Implications  
470 for dust and coal burning emission and secondary aerosol formation, *Atmospheric*  
471 *Chemistry and Physics*, 10, 6087-6096, 2010.

472 Wang, G., Kawamura, K., Umemoto, N., Xie, M., Hu, S., and Wang, Z.: Water-soluble organic  
473 compounds in PM<sub>2.5</sub> and size-segregated aerosols over Mt. Tai in North China Plain,  
474 *Journal of Geophysical Research-Atmospheres*, 114, D19208,  
475 [doi:10.1029/2008JD011390](https://doi.org/10.1029/2008JD011390), 2009.

476 Wang, G., Kawamura, K., Cao, J., Zhang, R., Cheng, C., Li, J., Zhang, T., Liu, S., and Zhao, Z.:  
477 Molecular distribution and stable carbon isotopic composition of dicarboxylic acids,  
478 ketocarboxylic acids and  $\alpha$ -dicarbonyls in size-resolved atmospheric particles from Xi'an  
479 city, China, *Environmental Science & Technology*, 46, 4783-4791, 2012.

480 Wang, G., Zhang, R., Zamora, M. L., Gomez, M. E., Yang, L., Hu, M., Lin, Y., Guo, S., Meng,  
481 J., Li, J., Cheng, C., Hu, T., Ren, Y., Wang, Y., Gao, J., Cao, J., An, Z., Zhou, W., Wang, J.,  
482 Marrero-Ortiz, W., Tian, P., Secrest, J., Peng, J., Du, Z., Zheng, J., Shang, D., Zeng, L.,  
483 Shao, M., Wang, W., Huang, Y., Wang, Y., Zhu, Y., Li, Y., Hu, J., Pan, B., Cai, L., Cheng,  
484 Y., Rosenfeld, D., Liss, P. S., Duce, R. A., Kolb, C. E., and Molina, M. J.: Persistent Sulfate  
485 Formation from London Fog to Chinese Haze, *Proceedings of National Academy of Science*  
486 *of United States of America*, 113(48), 13630-13635, [doi/10.1073/pnas.1616540113](https://doi.org/10.1073/pnas.1616540113),  
487 2016.

488 Wang, G. H., Niu, S. L., Liu, C., and Wang, L. S.: Identification of dicarboxylic acids and  
489 aldehydes of PM<sub>10</sub> and PM<sub>2.5</sub> aerosols in Nanjing, China, *Atmospheric Environment*,  
490 36(12), 1941-1950, 2002.

491 Wang, G. H., Kawamura, K., Watanabe, T., Lee, S. C., Ho, K. F., and Cao, J. J.: Heavy loadings  
492 and source strengths of organic aerosols in China, *Geophysical Research Letters*, 33,  
493 L22801, [doi:10.1029/2006GL027624](https://doi.org/10.1029/2006GL027624), 2006.

494 Wang, G. H., Zhou, B. H., Cheng, C. L., Cao, J. J., Li, J. J., Meng, J. J., Tao, J., Zhang, R. J., and  
495 Fu, P. Q.: Impact of Gobi desert dust on aerosol chemistry of Xi'an, inland China during  
496 spring 2009: differences in composition and size distribution between the urban ground  
497 surface and the mountain atmosphere, *Atmospheric Chemistry and Physics*, 13(2), 819-835,  
498 2013.

499 Wang, J., Wang, G., Gao, J., Wang, H., Ren, Y., Li, J., Zhou, B., Wu, C., Zhang, L., Wang, S.,  
500 and Chai, F.: Concentrations and stable carbon isotope compositions of oxalic acid and  
501 related SOA in Beijing before, during, and after the 2014 APEC, *Atmospheric Chemistry*

502 and Physics, 17(2), 981-992, 2017.

503 Wang, L., Lal, V., Khalizov, A.F., and Zhang, R.: Heterogeneous chemistry of alkylamines with  
504 sulfuric acid: Implications for atmospheric formation of alkylammonium sulfates,  
505 Environmental Science & Technology, 44, 2461–2465, 2010a.

506 Wang, L., Khalizov, A.F., Zheng, J., Xu, W., Lal, V., Ma, Y., and Zhang, R.: Atmospheric  
507 nanoparticles formed from heterogeneous reactions of organics, Nature Geoscience, 3, 238-  
508 242, 2010b.

509 Wang, Y., Zhang, Q., Jiang, J., Zhou, W., Wang, B., He, K., Duan, F., Zhan, Q., Philip, S., and  
510 Xie, Y.: Enhanced sulfate formation during China's severe winter haze episode in January  
511 2013 missing from current models, Journal Geophysical Research-Atmospheres, 119(17),  
512 10425-10440, doi:10.1002/2013JD021426, 2014.

513 Wexler, A.S., and Clegg, S. L.: Atmospheric aerosol models for systems including the ions  $H^+$ ,  
514  $NH_4^+$ ,  $Na^+$ ,  $SO_4^{2-}$ ,  $NO_3^-$ ,  $Cl^-$ ,  $Br^-$  and  $H_2O$ . Journal of Geophysical Research, 107 (D14),  
515 4207, doi:10.1029/2001JD000451, 2002.

516 Yao, L., Wang, M.-Y., Wang, X.-K., Liu, Y.-J., Chen, H.-F., Zheng, J., Nie, W., Ding, A.-J.,  
517 Geng, F.-H., Wang, D.-F., Chen, J.-M., Worsnop, D. R., and Wang, L.: Detection of  
518 atmospheric gaseous amines and amides by a high-resolution time-of-flight chemical  
519 ionization mass spectrometer with protonated ethanol reagent ions, Atmospheric Chemistry  
520 and Physics, 16(22), 14527-14543, 2016.

521 Yu, J. Z., Huang, X. F., Xu, J. H., and Hu, M.: When aerosol sulfate goes up, so does oxalate:  
522 Implication for the formation mechanisms of oxalate, Environmental Science & Technology,  
523 39(1), 128-133, 2005.

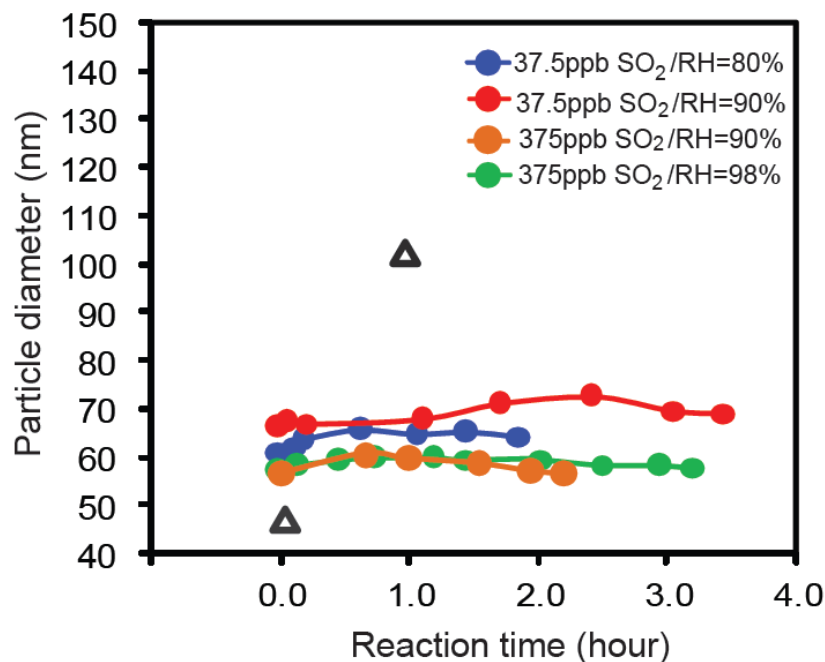
524 Zhang, R., Wang, G., Guo, S., Zamora, M. L., Ying, Q., Lin, Y., Wang, W., Hu, M., and Wang,  
525 Y.: Formation of urban fine particulate matter, Chemical Reviews, 115, 3803-3855,  
526 doi:10.1021/acs.chemrev.3805b00067, 2015.

527 Zhang, H., Chen, S., Zhong, J., Zhang, S., Zhang, Y., Zhang, X., Li, Z., and Zeng, X.C.:  
528 Formation of aqueous-phase sulfate during the haze period in China: Kinetics and  
529 atmospheric implications, Atmospheric Environment, 177, 93-99, 2018.

530 Zheng, J., Ma, Y., Chen, M., Zhang, Q., Wang, L., Khalizov, A. F., Yao, L., Wang, Z., Wang, X.,  
531 and Chen, L.: Measurement of atmospheric amines and ammonia using the high resolution  
532 time-of-flight chemical ionization mass spectrometry, Atmospheric Environment, 102, 249-  
533 259, 2015.

534  
535  
536

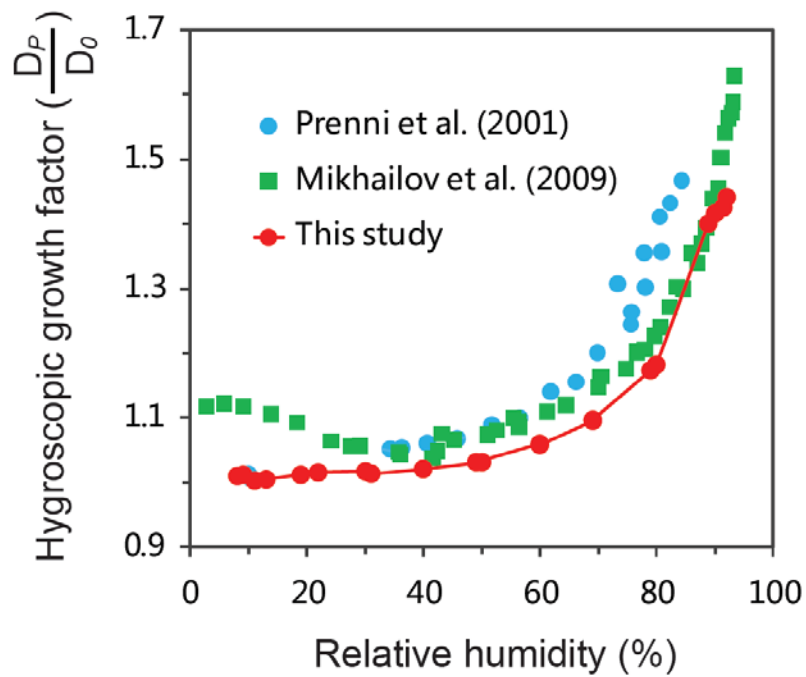
537  
538



539  
540  
541  
542  
543  
544  
545  
546  
547  
548  
549  
550  
551

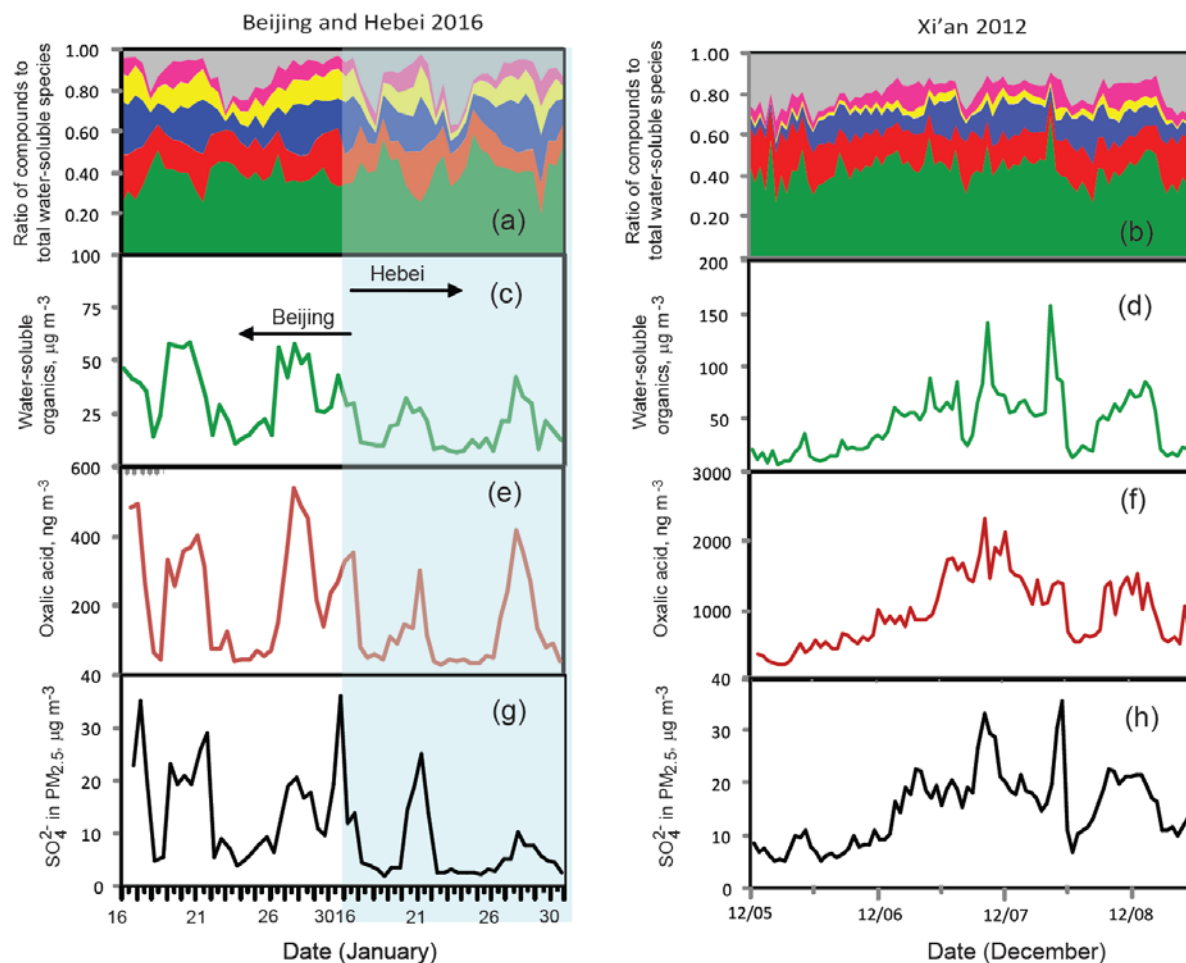
Figure 1. Size evolution of ammonium sulfate (circle dots) and oxalic acid (black triangles) particles after exposure to SO<sub>2</sub>, NO<sub>2</sub>, and NH<sub>3</sub> at different RH levels. Variations in mobility diameter ( $D_p$ ) of the particles as a function of reaction time. The symbols with different colors denote measurements with exposure to different SO<sub>2</sub>, NO<sub>2</sub> and NH<sub>3</sub> concentrations and RH levels. For the ammonium sulfate particles exposure experiment, two levels of SO<sub>2</sub> were used, which are 37.5 ppb and 375 ppb, respectively, while the NO<sub>2</sub> concentration is 375 ppb, and the NH<sub>3</sub> concentration is 500 ppb. For the oxalic acid particles exposure experiment, the SO<sub>2</sub> concentration is 250 ppb, the NO<sub>2</sub> concentration is 250 ppb, and the NH<sub>3</sub> concentration is 1 ppm (The data of oxalic acid growth are cited from the previous study by Wang et al (2016)).

552  
553



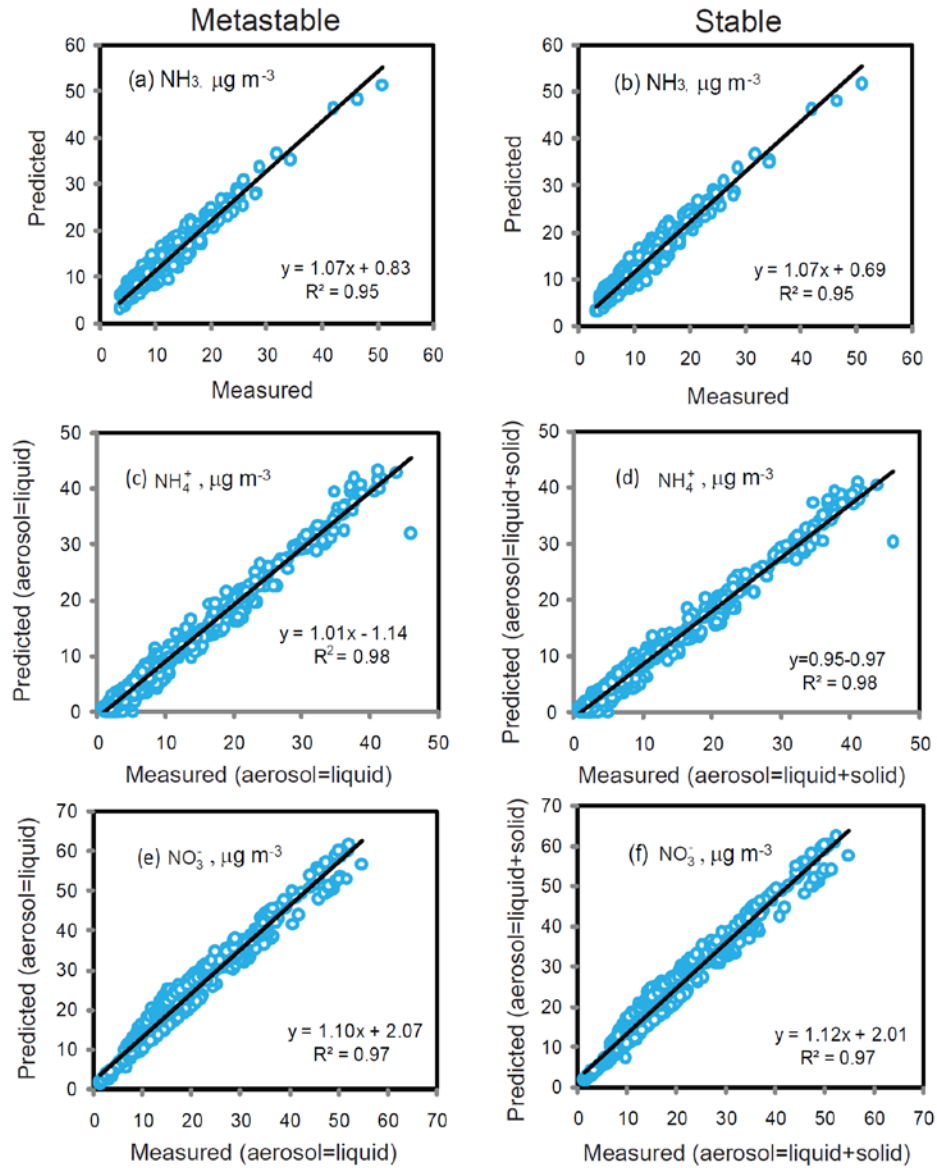
554  
555  
556 Figure 2. Measured hygroscopic growth factor (HGF) of oxalic acid particles at different RH  
557 conditions.  $D_p$  is the particle diameter at an elevated RH, and  $D_0$  (100nm) is the initial diameter  
558 of oxalic acid particles at RH = 8%.

559  
560  
561  
562  
563  
564



565  
 566  
 567  
 568  
 569  
 570  
 571  
 572

Figure 3. Measurements of water-soluble organic matter (WSOM) of  $PM_{2.5}$  collected in Beijing and Hebei Province during the winter of 2016 (left panels: a, c, e and g) and in Xi'an during the winter of 2012 (right panels: b, d, f and h). In (a) and (b), the green, red, blue, yellow, pink, and gray colors represent WSOM, sulfate, nitrate, ammonium, chloride, and the others (i.e., the sum of  $Na^+ + Ca^{2+} + Mg^{2+} + K^+$ ), respectively.



573

574 Figure 4. Comparison of measured  $\text{NH}_3$ ,  $\text{NH}_4^+$ , and  $\text{NO}_3^-$  concentrations with those predicted by  
 575 ISORROPIA-II model using the forward mode under the metastable (left panels) and stable  
 576 assumptions (right panels).  
 577